

## Potential Energy Surfaces for the Reaction $\text{Al} + \text{O}_2 \rightarrow \text{AlO} + \text{O}^\dagger$

Vincent Ledentu, Ali Rahmouni,<sup>‡</sup> Gwang-Hi Jeung,<sup>\*</sup> and Yoon Sup Lee<sup>§\*</sup>

*Chimie Théorique, Université de Provence, Case 521 (UMR6517), Campus de St-Jérôme, 13397 Marseille, France*

*<sup>‡</sup>Laboratoire de Modélisation et Méthodes de Calcul, Centre Universitaire Dr Moulay Tahar, Saida, Algeria*

*<sup>§</sup>Department of Chemistry and School of Molecular Sciences (BK21), Korea Advanced Institute of Science and Technology, Daejeon 305-701, Korea*

*Received May 10, 2004*

Potential energy surfaces for the reaction  $\text{Al} + \text{O}_2 \rightarrow \text{AlO} + \text{O}$  have been calculated with the multireference configuration interaction (MRCI) method using molecular orbitals derived from the complete active space self-consistent field (CASSCF) calculations. The end-on geometry is the most favourable for the reaction to take place. The small reaction barrier in the present calculation (0.11 eV) is probably an artefact related to the ionic-neutral avoided crossing. The charge analysis implies that the title oxidation reaction occurs through a harpooning mechanism. Along the potential energy surface of the reaction, there are two stable intermediates of  $\text{AlO}_2$  ( $C_{\infty v}$  and  $C_{2v}$ ) at least 2.74 eV below the energy of reactants. The calculated enthalpy of the reaction (-0.07 eV) is in excellent agreement with the experimental value (-0.155 eV) in part due to the fortuitous cancellation of errors in AlO and  $\text{O}_2$  calculations.

**Key Words :** Oxidation reaction. Harpooning mechanism. Reaction barrier. Covalent-ion coupling. Intermediates

### Introduction

The combustion of hydrogen and oxygen in the presence of light metal elements, like Li, Na, Mg, Al, has been considered as a potentially efficient rocket propulsion. Oxidation of those metals involves a complex mechanism and the final products cover a wide range of molecules. The solid form of AlO has many important industrial and technological applications, including recent one as a template for nano fabrication.<sup>1,2</sup> Pak and Gordon<sup>3</sup> have recently calculated the energy levels involved in the oxidation reaction of aluminium atom by *ab initio* methods and probed possible reaction pathways connecting those levels. The oxidation of aluminium atom has been recently studied by a crossed-beam laser-induced-fluorescence technique by Naulin and Costes<sup>4</sup> and Honma.<sup>5</sup> In these studies, the first step of oxidation is believed to lead to the AlO molecule and the oxygen atom in the ground state because they detected the  $B(^2\Sigma^-) \rightarrow X(^2\Sigma^-)$  transitions of AlO. Naulin and Costes' apparatus can continuously vary the angle between the Al and  $\text{O}_2$  molecular beams from  $\pi/2$  to  $\pi/8$ . By analysing the reactant kinetic energies, they have found the exothermicity of this reaction to be  $155 \pm 8$  meV (here 1 eV is equivalent to 23.06 kcal mol<sup>-1</sup> or 96.49 kJ mol<sup>-1</sup>). They have estimated a large reactive cross-section for the  $\text{Al}(^2P_{1/2})$ : 1.2 nm<sup>2</sup> for the kinetic energy of 6 meV, and 0.12 nm<sup>2</sup> for the kinetic energy of 155 meV. On the other hand, they have found a large difference of reactivity for the two spin-orbit states of aluminium, 1/2 and 3/2 at low collision energies, confirming a previous experimental<sup>6</sup> and theoretic-

cal<sup>7</sup> works. Naulin and Costes reported the  $^2P_{1/2}$  state to be 3 to 4 times more reactive than the  $^2P_{3/2}$  at the collision energy of 12 meV, but the difference decreased with the increasing collision energy. In Honma's apparatus, the two beams cross at the right angle, and the collision energies were varied by using different carrier gases. His observed rotational distributions of the AlO product for the two spin-orbit states were similar at two different relatively high collision energies.

In those experimental studies, the energy partition into various vibrational and rotational states showed a distribution occupying lower energy states than could be expected from the statistical picture, in agreement with old studies.<sup>8,9</sup> It appears that the oxidation involves the intermediate state whose lifetime is long enough to undergo several internal vibrations but too short for the complete relaxation.

In this work, we are interested in the reliable potential energy surface (PES) and the wave functions to understand the first step of the oxidation mechanism. Although several PES have been calculated in the past, it is difficult to attribute their accuracy. Pak and Gordon's calculation<sup>3</sup> showed indeed a large variation of the relative energy levels according to the methods employed. They have used the multiconfiguration self-consistent field (MCSCF) method to probe the PES to find the local minima and the transition states, then performed the coupled cluster singles and doubles with perturbed triples [CCSD(T)] and multi-reference configuration interaction (MRCI) calculations for the MCSCF optimized geometries. The title reaction involves an ionic-neutral surface crossing due to a charge transfer from the metal atom to the oxygen molecule, and it is always delicate to have a balanced description between the ionic and neutral components as will be explained in sections below.

<sup>†</sup>Dedicated to Professor Yong Hae Kim for his distinguished achievements in organic chemistry.

<sup>\*</sup>Co-Corresponding Authors. G.-H. Jeung (jeung@up.univ-mrs.fr), Y. S. Lee (yoonsuplee@kaist.ac.kr)

### Methods of Computation

We have optimized the atomic basis functions for aluminium and oxygen. For the aluminium atom, 17s12p7d Gaussian type orbitals (GTOs) were obtained to optimally describe the  $3s^2 3p$  ( $^2P^\circ$ ),  $3s^2 4s$  ( $^2S$ ), and  $3s^2 3d$  ( $^2D$ ) states in configuration interaction (CI) calculation. These were contracted to 14s10p5d atomic basis functions (ABFs). For oxygen atom, 12s7p3d GTOs were obtained for the  $2s^2 2p^4$  ( $^3P$ ) and ( $^1D$ ) states and the anion  $2s^2 2p^5$  ( $^2P^\circ$ ). These were contracted to 8s5p3d ABFs.

For the molecular calculations, we have performed two series of calculations initially, one set for the  $C_{\infty v}$  geometry and the other set for the  $C_{2v}$  geometry. Then we have done a third series of calculation for the  $C_s$  point group symmetry. We have used complete active space multi-configuration self-consistent field (CASSCF) calculations consisting of 9 valence electrons (one from Al and four from O) distributed in the six  $a'$  and three  $a''$  molecular orbitals (MOs) for the  $C_s$  point group symmetry, or the three  $\sigma$  and six  $\pi$  MOs for the  $C_{\infty v}$  symmetry, or the 3  $a_1$ , one  $a_2$ , three  $b_1$  and two  $b_2$  MOs for the  $C_{2v}$  geometry. The resulting MOs were used as the basis for the MRCI calculations. We have used the Molcas program package.<sup>10</sup>

### Results and Discussion

Various energy differences involved in the title reaction are reported in Table 1. Our calculated energy differences are in general in good agreement with the experimental data, except for the electron affinity of the oxygen atom which is much underestimated in our calculation. In fact, the electron affinity is one of the most difficult parts of the *ab initio* calculation. This results in the underestimation of the bond energy of ionic molecules as can be seen for the binding energy of AlO and  $O_2$  in Table 1. The bond strength of homopolar molecules such as the oxygen molecule is also affected due to the ion-pair resonance term. However, our calculated enthalpy of the title reaction happens to be quite good (0.07 eV, exothermic) in comparison to the experimental value (0.155 eV, exothermic) due to the fortuitous cancellation of error.

The potential energy section along the reactant channel studied in  $C_{\infty v}$  with the distance between two oxygen atoms fixed at 2.3 bohr is reported in Figure 1. The ionic-neutral avoided crossing region is very difficult to calculate and the *ab initio* calculation often leads to an overestimation of the

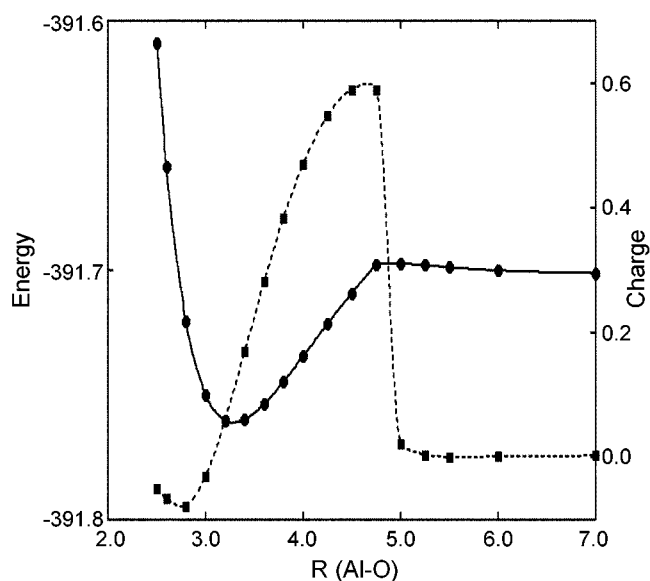


**Figure 1.** Potential energy (solid curve) and the effective charge of aluminium (broken curve) along the reactive part:  $R(\text{Al-O})$  with  $R(\text{O-O})$  fixed to 2.3 bohr (in atomic units).

reaction barrier height. Our calculated reaction barrier height for the title reaction is estimated to be 0.11 eV. Pak and Gordon<sup>3</sup> did not report the  $C_{\infty v}$  case, but presented the  $C_{2v}$  case, where they obtained the activation barrier whose height varies largely (0.04-0.13 eV) according to the method used. Our calculation for the  $C_{2v}$  case showed the potential barrier which is much higher than that in the  $C_{\infty v}$  case. This may be due to a stronger steric repulsion with the closed-shell  $O_2$  electron distribution in the  $C_{2v}$  geometry in comparison to the  $C_{\infty v}$  case. In contrast, Naulin and Costes<sup>4</sup> did not observe any reaction barrier for their lowest collision energy of 6 meV. Around the ionic-neutral avoided crossing region, there occurs a sudden electron transfer from the metal atom to the oxygen molecule as can be seen in Figure 1. This corresponds to a so-called harpooning.

The electron affinity of the oxygen molecule, calculated at the level of CI comparable to the one we used for the  $\text{AlO}_2$  complex is negative, while the experimental value estimated by the photoelectron detachment spectroscopy<sup>12</sup> is 0.451 eV. Considering the underestimation of the electron affinity for the oxygen atom and oxygen molecule, we think that the real ionic-neutral avoided crossing occurs in a larger intermolecular distance  $R(\text{Al-O}_2)$  so that the artificial reaction barrier mentioned above should disappear. The Mulliken population analysis of the  $\text{AlO}_2$  complex shows that about 2/3 of the electron spends time around the oxygen molecule.

The intermediate complex  $\text{AlO}_2$  is calculated to be very stable into any dissociation. The lowest energy is found for the  $C_{2v}$  geometry and the most stable  $C_{\infty v}$  geometry lies slightly higher in energy at the CASSCF level of calculation. The energy difference between these two isomers is too small to conclude which one is really more stable. However, while the reaction through the  $C_{\infty v}$  isomer leads to the product without a potential barrier other than the artificial

**Table 1.** Energy differences relevant to the title reaction, in eV

	This work	Experimental
I.P. (Al)	5.92	5.9858 <sup>a</sup>
E.A. (O)	0.85	1.461 <sup>b</sup>
$D_0$ (Al-O)	4.86	5.270 <sup>b</sup>
$D_0$ ( $O_2$ )	4.79	5.116 <sup>c</sup>
$\Delta H$	-0.07	-0.155 <sup>b</sup>

<sup>a</sup>From Ref. 11. <sup>b</sup>From Ref. 13. <sup>c</sup>From Ref. 14.

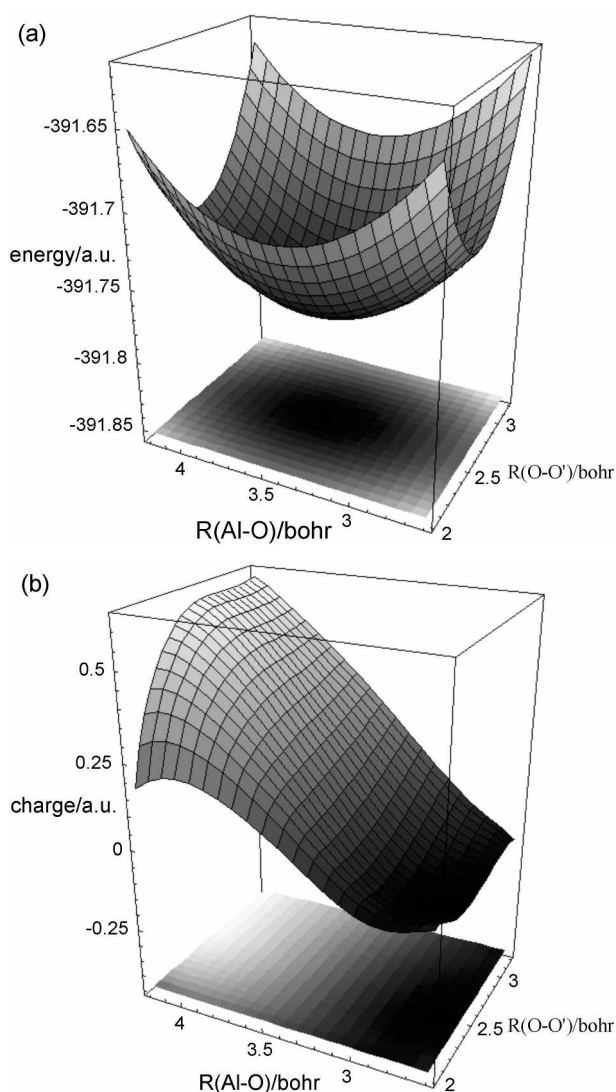


**Figure 2.** (a) Potential energy surface for the intermediate complex  $\text{AlO}_2$ . (b) Net charge of the aluminium atom in the  $\text{AlO}_2$  complex.

one mentioned above, the reaction passing through the  $\text{C}_{2v}$  isomer leads to a second barrier before reaching to the product. Subsequently, we did not attempt to optimize the  $\text{C}_{2v}$  geometry at the MRCI level. We have tried to locate the transition state to obtain the height of this second barrier, but were not able to overcome the divergence problem in CASSCF calculations. However, we have a substantial amount of data to presume that the transition state lies higher than the reactant level. As a result, we think that the title reaction cannot take place through the  $\text{C}_{2v}$  geometry but rather through a  $\text{C}_{\infty v}$  end-on geometry. The  $\text{C}_{\infty v}$  potential energy surface is drawn in Figure 2a. It shows a part of the potential well where the  $\text{AlO}_2$  complex is 2.74 eV below the energy level of reactants  $\text{Al} + \text{O}_2$ . The O-O distance in the minimum energy point is 1.32 Å that is slightly elongated with respect to the free oxygen molecule (1.208 Å), and the Al-O distance is 1.69 Å that is also slightly larger than that of the free  $\text{AlO}$  molecule (1.618 Å).

The effective charge of the aluminium atom shown in Figure 2b shows that the maximum charge transfer (the

highest region in this figure) does not coincide with the minimum energy geometry but to larger O-O and Al-O distances. The product section of the potential energy surface shows that the electron transferred to the oxygen molecule is principally localized to the bonding oxygen molecule (O) rather than the terminal oxygen atom (O'). Thus the reaction mechanism appears similar to the hydrogenation reaction of the alkali atom studied by our group.<sup>15,16</sup>

In summary, the end-on geometry is the most favourable for the reaction to take place. It is at the same time closer to the reactant and the product than the  $\text{C}_{2v}$  intermediate isomer. The small reaction barrier in the present calculation is probably an artefact related to the ionic-neutral avoided crossing. Our work clearly shows that the title oxidation reaction occurs through a harpoon mechanism. To study the dynamical aspect of the reaction, we need to do more accurate calculation and survey a large area of the potential energy surface. In particular, we have to know how the two isomers we have found so far ( $\text{C}_{\infty v}$  and  $\text{C}_{2v}$ ) are interconnected and which one is really lower in energy. Solving this problem requires to overcome the divergence problem around the ionic-neutral avoided-crossing region and to do more extensive configuration interactions.

**Acknowledgement.** This paper is dedicated to Professor Yong Hae Kim in recognition of his great contribution in science on the occasion of his official retirement from KAIST. This work was, in part, supported by CNRS and KOSEF (F01-2002-000-20094-0).

## References

1. Park, J. B.; Kim, Y.; Kim, S. K.; Lee, H. *Bull. Korean Chem. Soc.* **2004**, *25*, 563.
2. Yoon, C.; Suh, J. S. *Bull. Korean Chem. Soc.* **2002**, *23*, 1519.
3. Pak, M. V.; Gordon, M. *J. Chem. Phys.* **2003**, *118*, 4471.
4. Naulin, C.; Costes, M. *Chem. Phys. Lett.* **1999**, *310*, 231.
5. Honma, K. *J. Chem. Phys.* **2003**, *119*, 3641.
6. Chen, K.; Sung, C.; Chang, T.; Lee, K. *Chem. Phys. Lett.* **1995**, *240*, 17.
7. Reignier, D.; Stoeklin, S. D.; Le Picard, S. D.; Canosa, A.; Rowe, B. R. *J. Chem. Soc., Faraday Trans.* **1998**, *94*, 1681.
8. Dagdigian, P. J.; Cruse, H. W.; Zare, R. N. *J. Chem. Phys.* **1975**, *62*, 1824.
9. Pasternack, L.; Dagdigian, P. J. *J. Chem. Phys.* **1977**, *67*, 3854.
10. Version 4; Andersson, K.; Blomberg, M. R. A.; Fülcher, M. P.; Karlström, G.; Lindh, R.; Malmqvist, P.-Å.; Neogrady, P.; Olsen, J.; Roos, B. O.; Sadlej, A. J.; Schuz, M.; Seijo, L.; Serrano-Andrés, L.; Siegbahn, P. E. M.; Widmark, P.-O. Lund University: 1997.
11. Physical Reference Data from the NIST website (<http://physics.nist.gov/>).
12. Travers, M. J.; Cowles, D. C.; Ellison, G. B. *Chem. Phys. Lett.* **1989**, *164*, 449.
13. Andersen, T.; Haugen, H. K.; Hotop, H. *J. Phys. Chem. Ref. Data* **1999**, *28*, 1511.
14. Huber, K. P.; Herzberg, G.; *Molecular Spectra and Molecular Structure, Constants of Diatomic Molecules*; Van Nostrand Reinhold: New York, 1979; Vol. 4.
15. Lee, H. S.; Lee, Y. S.; Jeung, G.-H. *J. Phys. Chem. A* **1999**, *103*, 11080.
16. Jeung, G.-H.; Lee, H. S.; Kim, K. H.; Lee, Y. S. *Chem. Phys. Lett.* **2002**, *358*, 151.